Stress Control of an Evolving Strike-Slip Fault System during the 2010–2011 Canterbury, New Zealand, Earthquake Sequence

Richard Sibson,[1] Francesca Ghisetti,[2] and John Ristau[3]

INTRODUCTION

Large earthquakes within seismogenic crust are generally thought to require the pre-existence of large fault structures. Such fault structures appear to evolve by the progressive growth and amalgamation of smaller faults and fractures (Cowie and Scholz 1992). In the course of their evolution some components of an evolving fault system may be inherited from previous tectonic episodes while others may be newly formed in the prevailing tectonic stress field. With increasing displacement and amalgamation of sub-structures, fault structures tend to become "smoother," less complex, and perhaps weaker (Wesnousky 1988).

The 2010–2011 Canterbury earthquake sequence occurred within the upper crust of the South Island of New Zealand around 100 km southeast from the fast-moving (20–30 mm/yr) Alpine and Hope fault strike-slip components of the Pacific-Australia transform fault system linking into the southern Hikurangi Margin subduction zone (Figure 1). As of 15 July 2011, the sequence has included three major shocks: the M_w 7.1 Darfield earthquake (3 September 2010 UTC) followed by an M_w 6.2 event on 21 February 2011 UTC and an M_w 6.0 event on 13 June 2011 UTC, along with a rich aftershock sequence that includes 27 shocks with $M_w > 5.0$. Rupturing occurred on previously unrecognized faults that appear to be components of a highly segmented E-W structure concealed beneath alluvial cover and/or Neogene volcanics. Some subsurface information is, however, available from seismic reflection lines and gravity surveys (*e.g.*, Field *et al.* 1989).

Here we seek to demonstrate how this complex sequence has likely arisen through reactivation under the contemporary tectonic stress field of a mixture of comparatively newly formed and older inherited fault structures.

1. Department of Geology, University of Otago, P.O. Box 56, Dunedin 9054, New Zealand
2. Terrageologica, 129 Takamatua Bay Rd., RD1, Akaroa 7581, New Zealand
3. GNS Science, Te Pu Ao, P.O. Box 30-368, Lower Hutt, New Zealand

TECTONIC/GEOLOGIC SETTING

The 2010–2011 Canterbury earthquakes occurred within 30 ± 5 km thick continental crust belonging to the buoyant Chatham Rise plateau contained within the Pacific plate (Eberhart-Phillips and Bannister 2002). Local geology (Figure 2) comprises a basement of highly deformed Mesozoic Torlesse metagraywackes and their metamorphosed equivalents at greater depth, unconformably overlain by a Late Cretaceous–Neogene cover sequence up to 2.5 km thick (Forsyth *et al.* 2008). Polyphase deformation within this basement assemblage includes accretion, folding and thrusting along the Gondwana margin, extensional fault structures from Late Cretaceous rifting of the Zealandia microcontinent, and Neogene transpression across the Alpine fault system.

The cover sequence consists of Late Cretaceous–Paleogene terrestrial-marine sedimentary units (including varying thicknesses of Late Cretaceous Mt. Somers calc-alkaline volcanics and Eocene basalts) overlain by a regressive Miocene-Pliocene clastic sequence that contains the predominantly basaltic Late Miocene (11–6 Ma) Banks Peninsula volcanics. Thickness variations are partly attributable to deposition as a Late Cretaceous–Paleocene syn-rift sequence accompanying extensional rifting along the Gondwana margin, which imposed an extensive fault fabric within the basement (Laird and Bradshaw 2004). Neogene shortening has led to varying reactivation of these inherited fault systems. Over the area of the Canterbury Plains the older units are largely obscured by Pliocene and Quaternary alluvial gravels up to a few hundred meters thick (Forsyth *et al.* 2008).

CONTEMPORARY STRESS FIELD

Available evidence on the contemporary regional stress field in the central South island (Sibson *et al.*, forthcoming) comes from two principal sources summarized in Table 1: 1) stress inversions from earthquake focal mechanisms together with one breakout determination from the Galleon-1 borehole; and 2) axes of maximum contractional strain-rate derived

doi: 10.1785/gssrl.82.6.824

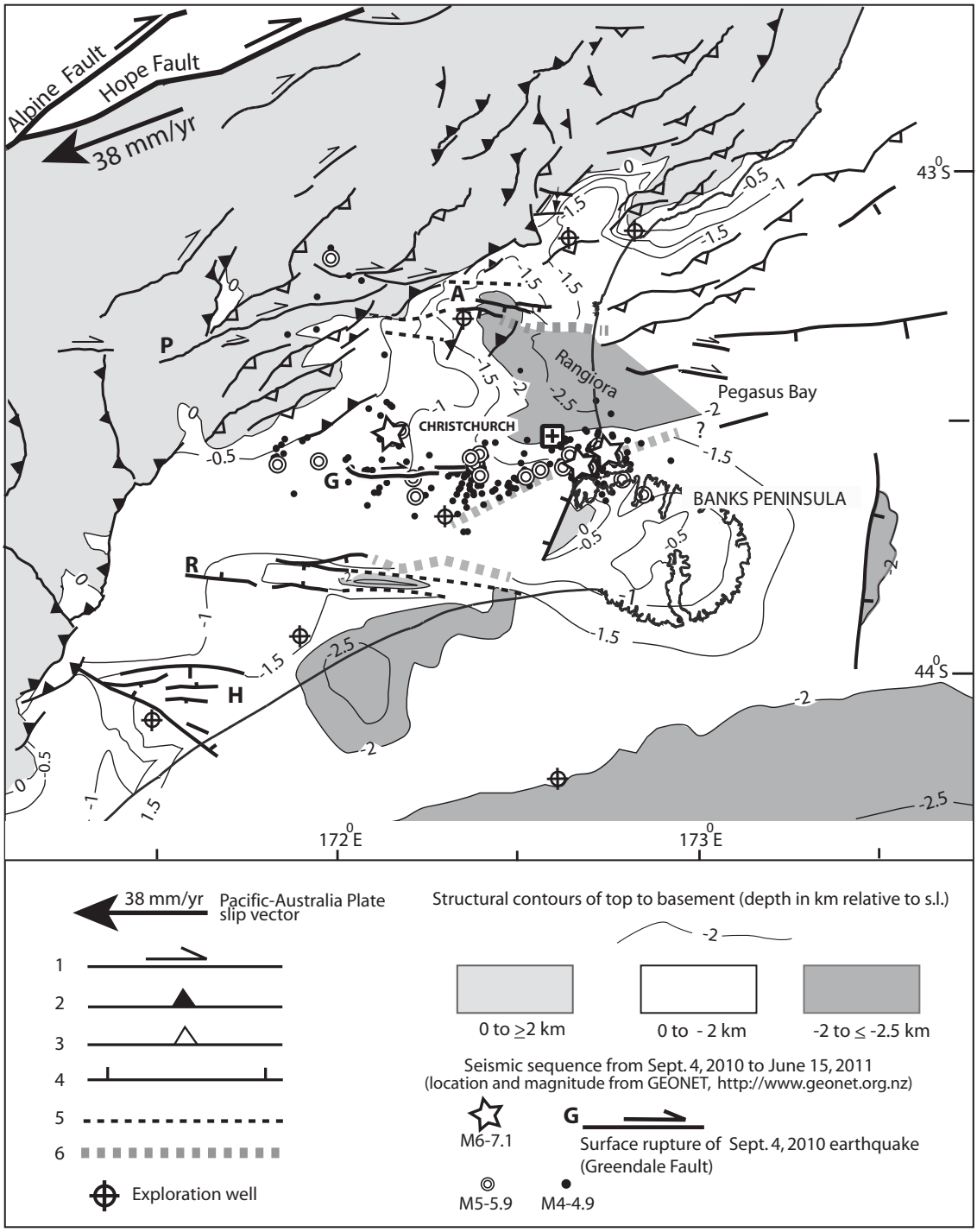

▲ **Figure 1.** Tectonic setting of the 2010–2011 Canterbury earthquake sequence. Mapped faults are from 1:250,000 geological maps (Forsyth 2001; Rattenbury *et al.* 2006; Cox and Barrell 2007; Forsyth *et al.* 2008). Offshore faults are from Barnes (1994), Mogg *et al.* (2008) and from preliminary data released from the 2011 offshore survey in the Pegasus Bay (NIWA and Otago University, http://www.gns.cri.nz/Home/News-and-Events/Media-Releases/Fault-structures-revealed). Subsurface geometry beneath the alluvial cover sequence of the Canterbury Plains and offshore is illustrated by the structural contours of depth to basement. Top of basement is modified from Hicks (1989) and Mogg *et al.* (2008) and incorporates basement depths in exploration wells, depth-converted seismic reflection lines (http://www.nzpam.govt.nz), and outcrop data. A, R, and H are respectively the Ashley, Rakaia, and Hinds fault systems, interpreted as inherited normal faults. P is the Porters Pass fault system and G is the right-lateral surface break of the 4 September 2010, M_w 7.1 earthquake on the Greendale fault (Quigley *et al.* 2010). 1) right-lateral faults; 2) W-dipping reverse faults (triangles in hanging wall); 3) E-dipping reverse faults (triangles in hanging wall); 4) normal faults (ticks in hanging wall); 5) inferred blind faults; 6) structurally controlled escarpment inferred from Bouguer gravity gradients from Bennett *et al.* (2000).

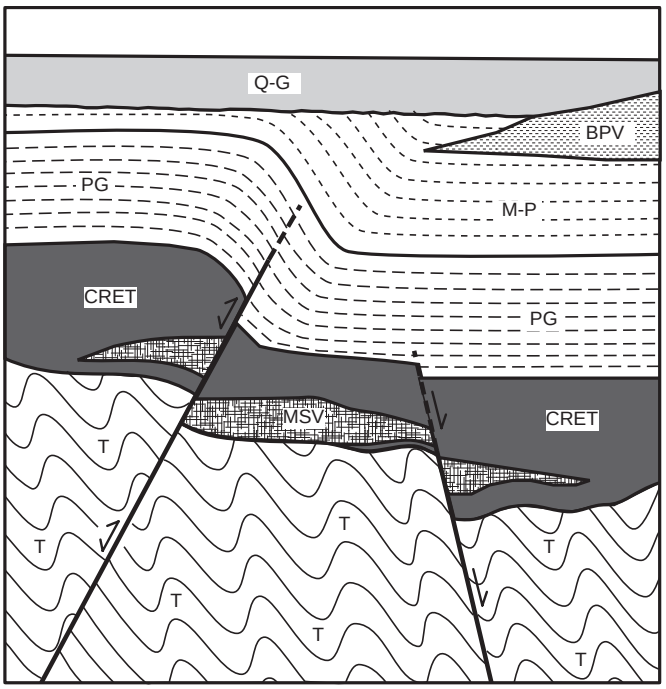

▲ **Figure 2.** Synoptic tectonostratigraphic column for the Canterbury Plains (not to scale). T = Torlesse basement assemblage; CRET = Late Cretaceous terrestrial sequence; MSV = Mt. Somers volcanics; PG = Paleogene marine sequence; M-P = Miocene-Pliocene marine-terrestrial sequence; BPV = Miocene Banks Peninsula volcanics; Q-G = Quaternary gravels.

from geodetic retriangulation and more modern GPS studies. Congruence between the two sources suggests a remarkably uniform regional stress field throughout the Canterbury region with maximum compressive stress σ_1 horizontal and oriented WNW-ESE (115° ± 5°). The apparent parallelism between σ_1 stress trajectories and maximum contractional strain-rate is explicable if the latter can be treated as a measure of maximum incremental shortening subparallel to σ_1 (cf. Keiding *et al.* 2009). This σ_1 orientation is also consistent with predominantly reverse-slip reactivation of structures trending NNE-NE along the Southern Alps range front. However, the dominance of strike-slip faulting in the Canterbury earthquake sequence suggests that the regional stress field is that of an "Andersonian" wrench (strike-slip) regime (Anderson 1905, 1951) with principal compressive stresses oriented: σ_1: 0°/115° ± 5°; σ_2: vertical; σ_3: 0°/025° ± 5°. Some local stress heterogeneity is, of course, to be expected, perhaps through buttressing by the Banks Peninsula volcanic edifice.

From the combination of strike-slip and reverse faulting throughout the region the likelihood is that the stress field is of the form $\sigma_1 > \sigma_v = \sigma_2 \sim \sigma_3$, with some local variance between $\sigma_v = \sigma_2$ and $\sigma_v = \sigma_3$. Brittle structures developing within the current "wrench" regime would be expected to have the orientations shown in the Figure 3 inset. Newly forming strike-slip faults should be vertical, lying at 25°–35° to σ_1 in accordance with the Coulomb criterion (Anderson 1905). Note that this also reflects the optimal attitude for reactivating existing faults over a broad range of sliding friction ($0.8 > \mu_s > 0.4$) (Sibson 1985). Grain-scale microcracks and macroscopic extension fractures would be statistically aligned perpendicular to σ_3 with an orientation 115° ± 5°/V. Planes of maximum shear stress controlling the orientation of subvertical ductile shear zones at depth below the seismogenic zone should lie at ±45° to σ_1 along trends of 070° (dextral) and 160° (sinistral).

PRINCIPAL COMPONENTS OF THE SEQUENCE

The principal components of the 2010–2011 Canterbury earthquake sequence are summarized in a seismotectonic cartoon illustrating the relationship of the different structures to the inferred σ_1 stress trajectories (Figure 3). Regional CMT mechanisms for $M_w \geq 4.0$ shocks within the sequence are illustrated in Figure 4. The sequential development and structural characteristics of the larger ruptures are discussed below.

TABLE 1
Stress Indicators in Canterbury, Central South Island (see also Sibson *et al.*, forthcoming).

Region	Method	σ_1 azimuth	Reference
Stress Determinations			
North Canterbury-Marlborough	Inversion of focal mechanisms	115 ± 16°	Balfour *et al.* 2005
Epicentral area 1994 Arthur's Pass M_w 6.7	Inversion of aftershock focal mechanisms	118 ± 4°	Robinson and McGinty 2000
Central S. Alps	Inversion of focal mechanisms	110 – 120°	Leitner *et al.* 2001
Offshore S. Canterbury	Borehole breakouts	114 ± 9°	Sibson *et al.* 2012
Maximum Contractional Strain Rates			
Okarito west of Alpine F.	Determination from repeated triangulation	117 ± 6°	Pearson 1994
Godley Valley east of Alpine F.	Determination from repeated triangulation	116 ± 14°	Pearson 1994
Canterbury Plains NW of ChCh	Determination from GPS campaigns	116 ± 9°	Pearson *et al.* 1995
Central Southern Alps	Determination from GPS campaigns	105 – 115°	Beavan and Haines 2001
Canterbury-Otago block	Rotating elastic block model	110 ± 8°	Wallace *et al.* 2007

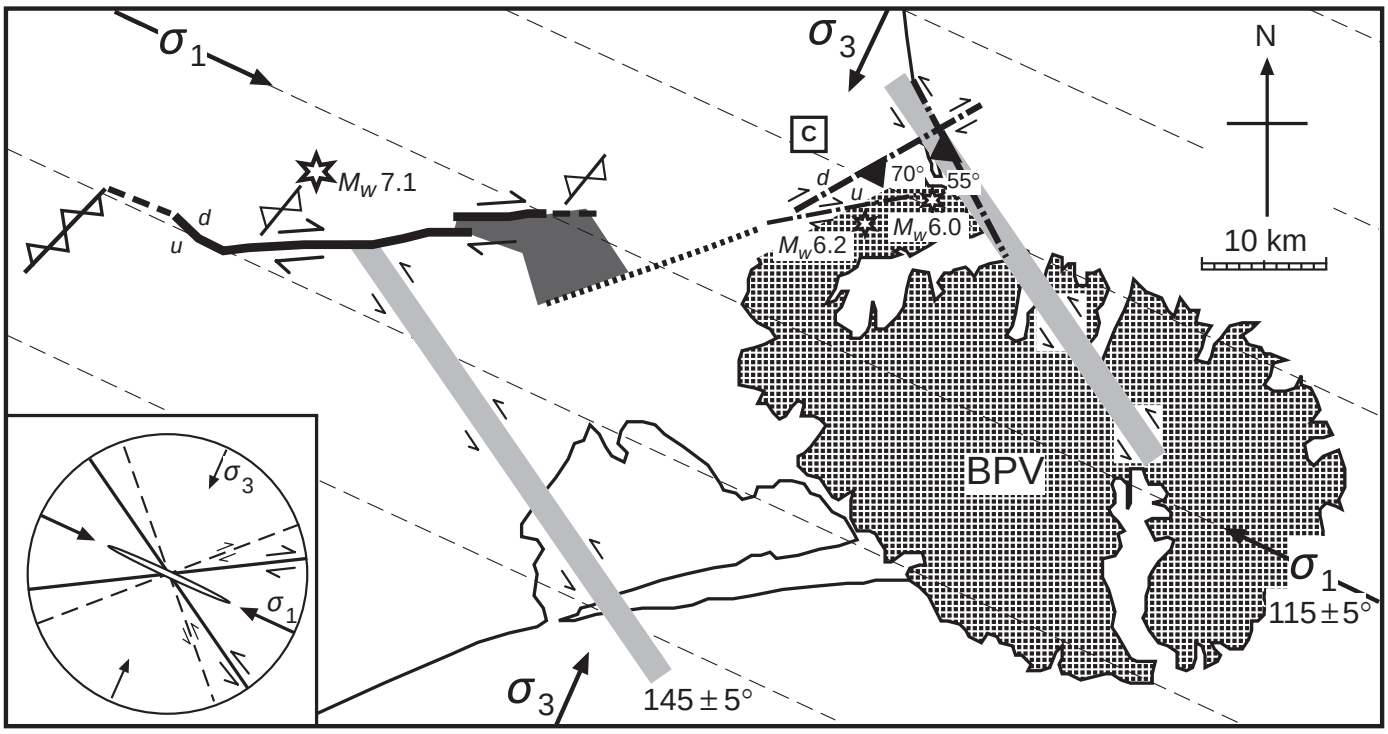

▲ **Figure 3.** Seismotectonic cartoon of the 2010–2011 Canterbury earthquake sequence in relation to the surface outcrop of Banks Peninsula volcanics (BPV), central Christchurch city (C), and the inferred regional stress field. Expected orientations of newly formed structures (ellipse = extension fracture; solid lines = Coulomb shears; dashed lines = ductile shears) shown in inset at lower left. Epicenters of major shocks denoted by stars; thick bold line = Greendale fault surface rupture; thinner dash-dot lines with filled teeth indicating dip direction = subsurface fault models for the M_w6.2 and M_w6.0 aftershocks (Beavan *et al.* 2011, page 789 of this issue); dotted line = microearthquake lineament; dark shading = area of intense aftershock activity in dilational stepover; gray-shaded bands = aftershock lineaments; hollow-toothed lines = belt of reverse-slip aftershocks (dip unconstrained).

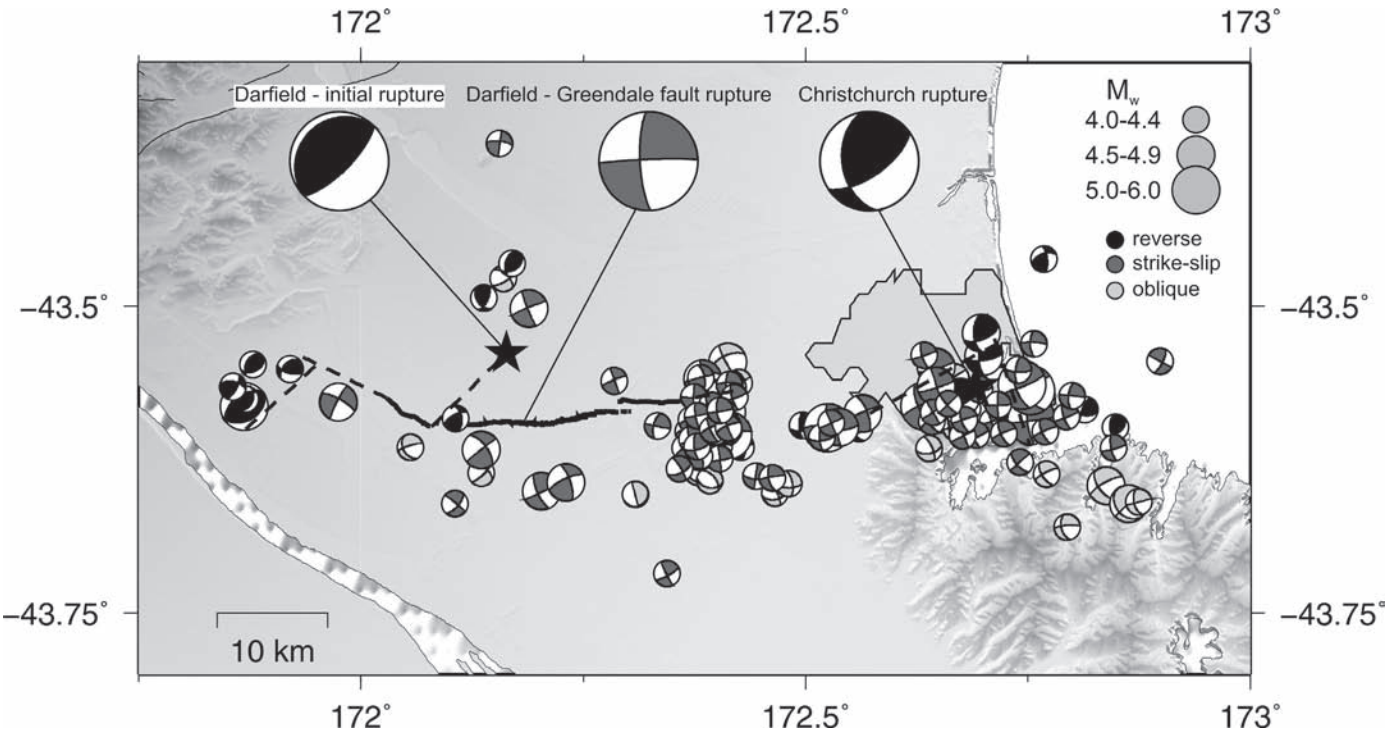

▲ **Figure 4.** Regional CMT focal mechanisms for M_w > 4.0 shocks within the 2010–2011 Canterbury earthquake sequence.

The 2010 M_w7.1 Darfield mainshock (16:35:46 on 3 September 2010 UTC) appears to be a composite rupture that initiated at a depth of 11 km below the Canterbury Plains, ~ 6 km north of a segmented surface rupture with dextral strike-slip < 5 m that developed during the earthquake and was mapped for nearly 30 km west-east across the plains (Quigley *et al.* 2010). This rupture, on what is now termed the Greendale fault (Figures 1 and 3), occurred in an extremely low-relief area of the plains without any prior topographic expression of the structure. Measured dextral displacements averaging 2.5 m but ranging up to ~ 5 m were consistent with pure strike-slip on a subvertical fault with an enveloping surface for the left-stepping rupture segments striking ~ 085°. While near-field focal mechanism and geodetic analyses suggest that initial rupturing involved reverse-slip on NE-SW striking planes (Gledhill *et al.* 2011; GeoNet regional moment tensor solution catalogue http://www.geonet.org.nz/resources/earthquake/), teleseismic analyses from long-period waves (USGS, http://earthquake.usgs.gov; Global CMT Project, http://www.globalcmt.org/CMTsearch.html) yield moment tensor mechanisms consistent with near-vertical dextral strike-slip on a rupture paralleling the mapped surface trace of the Greendale fault (Figure 4). Aftershocks, largely restricted to the upper crust at depths less than 12 km, were initially concentrated in an E-W swath around the surface rupture trace of the Greendale fault, though a number of subsidiary clusters and lineaments are also evident (Bannister *et al.* 2011, page 839 of this issue; Gledhill *et al.* 2011).

An aftershock cluster dominated by reverse-slip events abuts the Southern Alps foothills west and south of the western curving termination of the Greendale fault surface rupture (Figures 3 and 4). A strong subsidiary belt of activity with a mixture of strike-slip and reverse-slip mechanisms trends NNW from the mainshock epicenter toward the foothills and the Porters Pass system of strike-slip faults. Of particular structural interest is a diffuse aftershock lineament trending 145°–155° that developed south of the surface rupture in the first two weeks of the sequence and extended out to the coast and beyond. A strong concentration of activity including five of the M_w > 5.0 events is associated with the eastern end of the Greendale fault rupture and the area just south of it. From the mixture of strike-slip and normal fault mechanisms localized within this rhomboidal area of distributed activity (Gledhill *et al.* 2011), it appears to represent a dilational stepover to an en échelon ENE-trending aftershock lineament that extended eastward along the Banks Peninsula volcanic rangefront. Dilational stepovers (jogs) of this kind are well known for focusing long-continued aftershock activity with delayed slip transfer to the en échelon fault segment (Sibson 1986).

On 22 February (23:51:42 on 21 February 2011 UTC) central and eastern Christchurch were devastated by an M_w 6.2 aftershock located along the dominant ENE lineament following the northern outcrop margin of the Banks Peninsula volcanics. No surface fault break was observed, but Beavan *et al.* (2011, page 789 of this issue) modeled GPS and SAR data on surface deformation, in terms of dextral-reverse slip of up to 3 m on a buried rupture with a length of 12 km and a width of 7 km oriented ~060°/70° SE and extending to within 1 km of the surface beneath the Heathcote-Avon estuary (cf. Barnhart *et al.* 2011, page 815 of this issue). Beavan *et al.* (2011, page 789 of this issue) also suggest subsidiary strike-slip rupturing on a plane oriented ~ 080°/87° S (Figure 3). Aftershock activity was concentrated in the hanging wall of the main rupture, extending a little out to sea north and east of Banks Peninsula (Bannister *et al.* 2011, page 839 of this issue).

A further M_w6.0 aftershock occurred on 13 June (02:20:50 on 13 June 2011 UTC) with an epicenter some 5 km further to the ENE but again without surface rupture. The regional CMT solution yielded nodal planes suggesting either dextral-reverse slip on a fault oriented 068°/84° SSE, or sinistral-reverse slip on 161°/67° WSW with the slip vector raking 6° SSE (GeoNet catalog; http://www.geonet.org.nz). Support for this latter rupture orientation comes from an aftershock lineament that extended progressively along a trend of 140°–150°, subparallel to the SE-SSE trending lineament from the Greendale fault rupture (Figures 3 and 4). A "single-fault" interpretation of surface deformation recorded by GPS and DinSAR (J. Beavan, personal communication 2011) suggests left-reverse oblique slip of up to 1.5 m on a rupture plane oriented 155°/55° SW that extends from 1 km to 9 km in depth and along strike for ~ 14 km, cutting across the eastern end of the 22 February rupture.

BASEMENT FAULT FABRIC

Known fault traces extending into the basement (including Late Quaternary–Holocene active segments) identified by surface mapping in the Canterbury region and from seismic profiling, both onshore and offshore (Forsyth *et al.* 2008; Barnes 1994) (Figure 1) are clustered in two dominant groups based on their displacement characteristics (Figure 5).

1. Faults possessing dominant right-lateral components in the rangefront and foothills of the Southern Alps are subvertical, and oriented across the azimuthal range 050°–100° (Figure 5). ENE faults cluster along the active Porters Pass system, and E-W faults are mainly represented by the new rupture trace along the Greendale fault (Figure 1). Dominant orientations at 070°–100° are also shown by faults with components of normal separation, together with normal fault escarpments inferred from gradients in Bouguer gravity with surface traces indicating high-angle dips (70°–80°) to the north and south.
2. Faults dominated by reverse-slip include two groups of opposite-facing structures: 000°–050° trending faults dipping west, and 035°–090° trending faults dipping southeast (Figures 1 and 5). North-trending reverse faults dipping at moderate angles (40°–60°) to the west are well developed along the S. Canterbury rangefront (Figure 1). ENE-trending reverse faults dipping south at high angles (60°–70°) occur only in the north of the Canterbury region (Figure 1). Both groups include Quaternary-active segments.

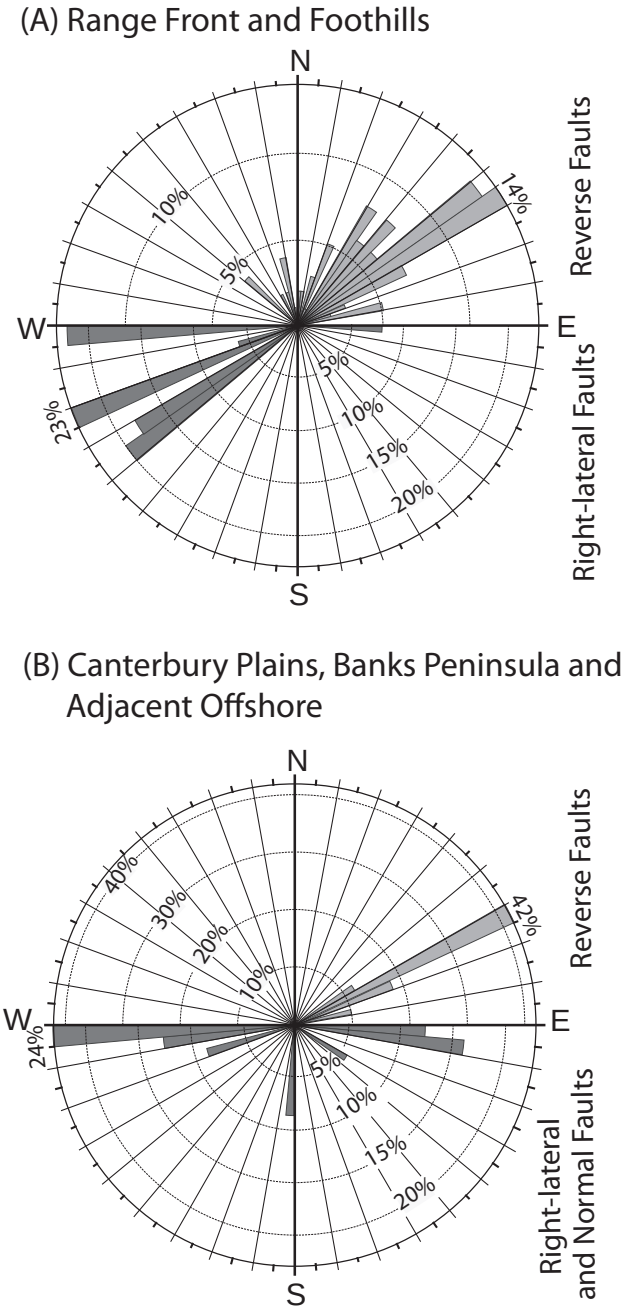

▲ **Figure 5.** Rose diagrams of fault strike azimuths within the Canterbury region covered by Figure 1, weighted for mapped length: A) Area of the Southern Alps rangefront and foothills where Torlesse basement is exposed; B) Area of the Canterbury Plains, Banks Peninsula, and offshore where basement is largely concealed. Top half of each plot is for faults where reverse-slip is dominant; bottom half is for faults with predominantly right-lateral and/or normal slip.

Offshore, the northwestern edge of the Chatham Rise preserves a strong extensional fabric defined by closely spaced E-W striking, S-dipping normal faults that bound half-grabens infilled with up to 2 km of inferred Late Cretaceous syn-rift sediments (Barnes 1994). Projection of these structures westward below the Canterbury Plains is conjectural but is based on Bouguer gravity anomalies (Hicks 1989; Bennett *et al.* 2000) together with information from exploration wells and seismic lines. These data have been used to contour the top of basement below the cover sequence (Figure 1). Two major depocenters (Pegasus-Rangiora basin to the north and Rakaia-Hinds basin to the south) are identified elongated in an easterly orientation and separated by an intervening structural high coincident with Banks Peninsula, where uplifted basement graywackes are exposed beneath the Miocene volcanics. Exploration wells have penetrated late syn-rift sequences infilling these basins. Discontinuous E-W fault traces mapped in the Quaternary gravels of the Canterbury Plains along the Ashley, Rakaia, and Hinds fault systems (Figure 1) are thus interpreted as surface traces of buried basement faults belonging to the structural domain of the Chatham Rise.

STRUCTURAL ANALYSIS

Observed slip senses on the three major ruptures within the earthquake sequence are consistent with the inferred pattern of σ_1 stress trajectories (Figure 3). However, some stress heterogeneity is evident, especially near rupture terminations and fault intersections (Figure 4). In Anderson's (1905, 1951) application of the Coulomb criterion for brittle shear failure to the initiation of faults within intact isotropic crust, strike-slip faults forming in a wrench stress regime ($\sigma_v = \sigma_2$) should be vertical and lie at $\pm$ ~30° to the σ_1 orientation. In contrast, large-displacement strike-slip faults commonly lie at far higher angles (often >45°) to regional σ_1 trajectories and are distinctly "non-Andersonian" (Mount and Suppe 1987; Balfour *et al.* 2005). It follows that vertical, low-displacement strike-slip faults at Andersonian orientations are possibly newly formed structures in the contemporary stress field, but they could also be inherited faults that happen to be optimally oriented for frictional reactivation. Following the same argument, oblique-slip ruptures most likely result from the reactivation of inherited faults in the prevailing stress field.

The principal ruptures of the Canterbury earthquake sequence can be viewed with these considerations in mind (Figure 3). First, the subvertical Greendale fault rupture lying at 25°–35° to regional σ_1 is at optimal Andersonian orientation, implying that it is either a comparatively newly formed strike-slip fault or an inherited structure that is optimally oriented for reactivation in the present stress field. It should be borne in mind that most of the inherited dip-slip faults within the basement are likely to have dips that are substantially less than vertical, though the Greendale rupture could occupy an amalgam of opposite-dipping structures. Note further, however, that at its western termination, the Greendale rupture trace curves into parallelism with the σ_1 stress trajectories (Figure 3), a propagation characteristic of low-displacement shear fractures and consistent with the local existence of CMT mechanisms with components of normal slip. Moreover, total strike-slip displacement on the Greendale fault appears not to be large because it has not been recognized to continue along strike into the bedrock geology of the Southern Alps foothills. In fact, at its

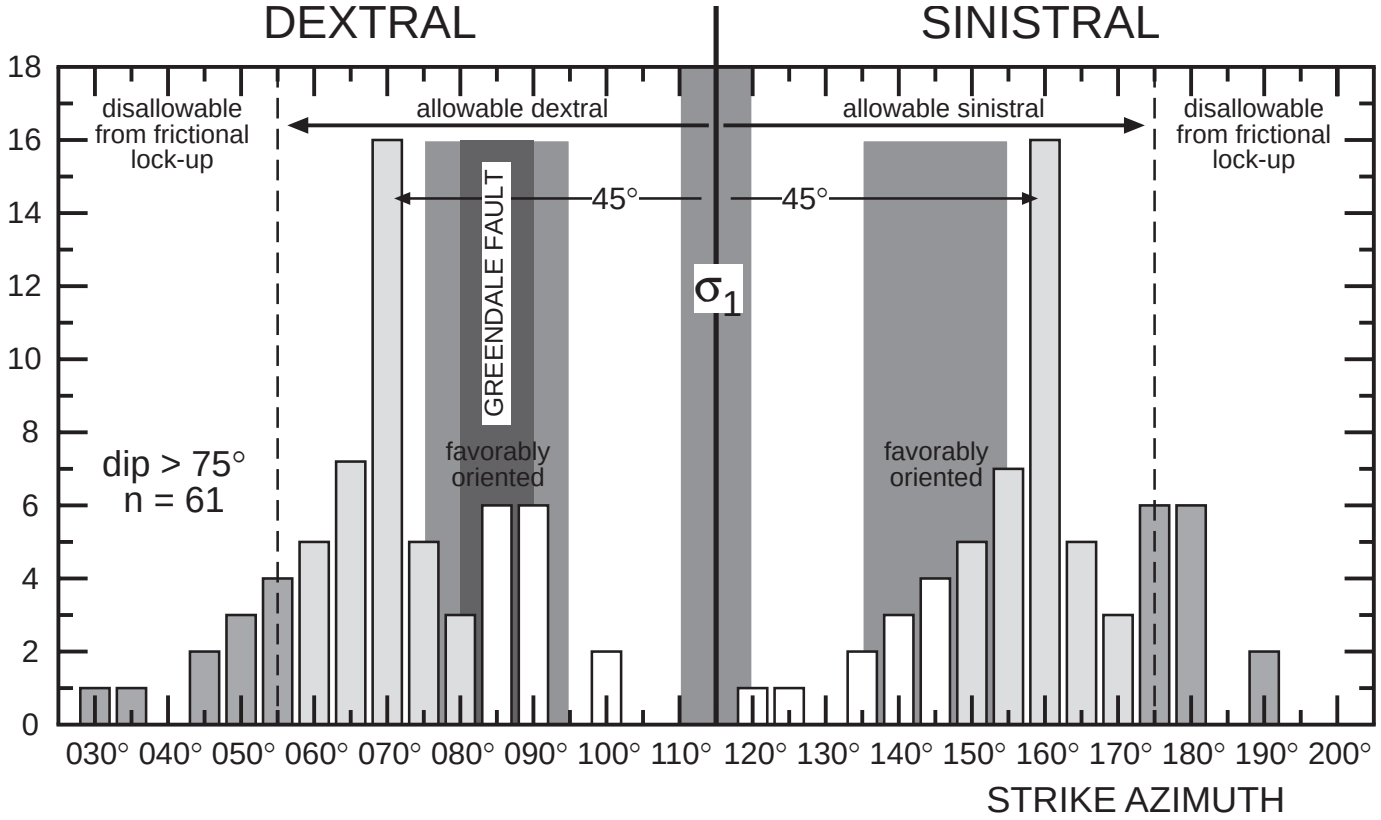

▲ **Figure 6.** Azimuthal distribution of nodal plane strikes for close-to-pure strike-slip CMT focal mechanisms (both planes dipping >75°) from the Canterbury earthquake sequence (GeoNet catalog http://www.geonet.org.nz), shown in relation to the inferred σ_1 direction.

western termination the fault appears to transform into local areas of normal faulting to the north and reverse faulting to the south (Figure 4).

While the dominant rupture in the 22 February aftershocks clearly involves dextral-reverse oblique slip, the subordinate subvertical plane (080°/87° S) lying subparallel to the Greendale fault (Beavan *et al.* 2011, page 789 of this issue) is at close to the ideal Andersonian orientation for strike-slip. This part of the sequence may therefore represent competition between inherited and newly formed fault segments. The two diffuse aftershock lineaments trending 140°–155° (Figure 3) are appropriately oriented for left-lateral strike-slip on vertical faults conjugate to the right-lateral Greendale fault with which they form a dihedral angle of ~ 50°–70°. Combining the CMT focal mechanism (161°/67° WSW) with the fault model for the 13 June M_w 6.0 aftershock (153°/55° SW) suggests predominantly left-lateral strike-slip on a moderately-to-steeply dipping plane with the slip vector raking only 6°, not too dissimilar to the ideal Andersonian relationship. However, the suggestion of a nonvertical rupture with a degree of oblique slip makes it likely that rupturing involved the reactivation of an inherited basement structure. These arguments are explored further by examining the distribution of strike azimuths, with respect to the inferred σ_1 direction, of aftershock nodal planes for close-to-pure strike-slip CMT focal mechanisms (GeoNet catalog, http://www.geonet.org.nz) where both nodal planes dip >75° (Figure 6). Because of the ambiguity as to which nodal plane represents the rupture plane, the distribution repeats at 90° intervals, separating potential dextral from potential sinistral strike-slip faults. Theoretical and field studies suggest that faults containing the σ_2 direction undergo frictional lock-up at 55°–60° to σ_1 (Collettini and Sibson 2001), reducing the allowable range of strike-slip fault orientations. Potential strike-slip orientations are thus reduced to three categories: dark-shaded columns are inadmissible because of frictional lock-up; light-shaded columns are positively discriminated as either dextral or sinistral strike-slip ruptures; and moderate-shaded columns could represent either dextral or sinistral strike-slip. Several features of the distribution are notable. First, despite its length and continuity, the Greendale fault trend is not dominant in strike-slip aftershock orientations. Moreover, a significant proportion of the positively discriminated mechanisms involve sinistral strike-slip on faults that commonly strike 135°–145°, conjugate to the dextral Greendale fault. However, by far the dominant azimuthal trend is 070° and/or 160°. Note first that these trends lie at ±45° to inferred σ_1 defining the orientations of vertical planes with maximum shear stress, the expected orientation for ductile shear zones developing in the basement below the brittle seismogenic crust (Figure 3). However, the 070° trend also lies subparallel to the Hope fault and the present interplate slip vector, suggesting the possibility of some kinematic control.

DISCUSSION

The 2010–2011 Canterbury earthquake sequence developed within a segmented fault system under an Andersonian wrench stress regime (σ_1: 0°/115° ± 5°; σ_2: vertical; σ_3: 0°/025° ± 5°) (Figure 3). Rupturing predominantly involved dextral strike-slip on subvertical E-W faults with varying degrees of reverse-slip on differently oriented (mostly ENE-WSW) fault segments. Local normal and reverse slip faulting also occurred at stress heterogeneities at strike-slip rupture tips. Some ruptures clearly involve reactivation of inherited basement faults but other comparatively low-displacement structures may be newly formed within the contemporary stress field.

Subordinate SE-SSE trending aftershock lineaments appear to represent a set of predominantly left-lateral strike-slip faults conjugate to the main dextral structures (Figure 3). The intersection angle of 50°–70° between the conjugate fault sets (±25°–35° to inferred σ_1) is consistent with Andersonian frictional fault mechanics. Note that this Andersonian conjugate relationship differs from the orthogonal relationship recognized for conjugate strike-slip faults in central Honshu, Japan, and southern California, which possibly reflects control of the active brittle structures by orthogonal ductile shear zones in the basement (Thatcher and Hill 1991).

Analysis of the strike-slip focal mechanisms from the Canterbury sequence (Figure 6) suggests that the subordinate set of steep sinistral strike-slip faults may be quite widespread. This has significance for rupture segmentation because sinistral displacements along the conjugate faults will create contractional jogs that impede slip along the main E-W dextral faults. In this regard, the 2010–2011 Canterbury sequence has similarities to the 2000 Western Tottori earthquake sequence in southwestern Honshu. The Western Tottori M_w 6.7 mainshock involved sinistral rupturing along a previously unrecognized NNW-SSE strike-slip fault, but high-resolution aftershock mapping showed the mainshock lineament to be offset in a series of contractional jogs by Andersonian conjugate dextral faults (Fukuyama *et al.* 2003). As in the Canterbury sequence, such contractional jogs may act as high-strength asperities because ruptures bypassing them likely have to break through comparatively intact rock. It is notable that particularly high apparent stresses and ground accelerations are associated with the intersection zone at the eastern end of the main E-W aftershock distribution in the Canterbury sequence where the 22 February M_w 6.2 rupture is apparently cross-cut by the 13 June M_w 6.0 rupture (Fry and Gerstenberger 2011, page 833 of this issue).

Overall, the fault system responsible for the Canterbury earthquake sequence appears to be controlled by the orientation of the tectonic stress field in the upper crust rather than conforming with local plate boundary kinematics. On this basis the earthquakes can be regarded as intraplate events remote from the main Alpine-Marlborough fault system defining the onshore plate boundary. Continuance of conjugate faulting has the important implication that displacement weakening leading to preferential failure has not yet reached the stage where one of the fault sets has become totally dominant and superseded the other. Amalgamation of inherited and newly formed fault components of low total displacement, together with segmentation from the cross-cutting of the major E-W dextral structures by conjugate left-lateral faults, has led to a rough, immature fault system capable of generating high stress-drop ruptures.

ACKNOWLEDGMENTS

The writers extend their thanks and appreciation to John Beavan, Stephen Bannister, and Martin Reyners for much helpful discussion and advice.

REFERENCES

Anderson, E. M. (1905). The dynamics of faulting. *Transactions of the Edinburgh Geological Society* **8**, 387–402.

Anderson, E. M. (1951). *The Dynamics of Faulting and Dyke Formation with Application to Britain*. 2nd ed. Edinburgh: Oliver & Boyd, 206 pp.

Balfour, N. J., M. K. Savage, and J. Townend (2005). Stress and crustal anisotropy in Marlborough, New Zealand: Evidence for low fault strength and structure-controlled anisotropy. *Geophysical Journal International* **163**, 1,073–1,086.

Bannister, S., B. Fry, M. Reyners, J. Ristau, and H. Zhang (2011). Fine-scale relocation of aftershocks of the 22 February M_w 6.2 Christchurch earthquake using double-difference tomography. *Seismological Research Letters* **82**, 839–845.

Barnes, P. M. (1994). Continental extension of the Pacific plate at the southern termination of the Hikurangi subduction zone: The North Mernoo fault zone, offshore New Zealand. *Tectonics* **13**, 753–754.

Barnhart, W., M. J. Willis, R. B. Lohman, and A. Melkonian (2011). InSAR and optical constraints on fault slip during the 2010–2011 New Zealand earthquake sequence. *Seismological Research Letters* **82**, 815–823.

Beavan, J., E. Fielding, M. Motagh, S. Samsonov, and N. Donnelly (2011). Fault location and slip distribution of the 22 February 2011 M_W 6.2 Christchurch, New Zealand, earthquake from geodetic data. *Seismological Research Letters* **82**, 789–799.

Beavan, J., and J. Haines (2001). Contemporary horizontal velocity and strain-rate fields of the Pacific-Australia plate boundary zone through New Zealand. *Journal of Geophysical Research* **106**, 741–770.

Bennett, D., R. Brand, D. Francis, S. Langdale, C. Mills, B. Morris, and X. Tian (2000). Preliminary results of exploration in the onshore Canterbury Basin, New Zealand. *New Zealand Petroleum Conference Proceedings*, 19–22 March 2000. Wellington, NZ: Crown Minerals, 12 pp. http://www.nzpam.govt.nz/cms/petroleum/conferences/conference-proceedings-2000.

Collettini, C., and R. H. Sibson (2001). Normal faults, normal friction? *Geology* **29**, 927–930.

Cowie, P., and C. H. Scholz (1992). Growth of faults by accumulation of seismic slip. *Journal of Geophysical Research* **97**, 11,085–11,095.

Cox, S. C., and D. J. A. Barrell (2007). *Geology of the Aoraki Area*. Institute of Geological and Nuclear Sciences 1:250,000 geological map 15, 1 sheet and 71 pp. Lower Hutt, New Zealand: GNS Science.

Eberhart-Phillips, D., and S. Bannister (2002). Three-dimensional crustal structure in the Southern Alps region of New Zealand from inversion of local earthquake and active source data. *Journal of Geophysical Research* **107**; doi:10.1029/2001JB000567.

Field, B. D., G. H. Browne, B. Davy, R. H. Herzer, R. H. Hoskins, J. L. Raine, G. J. Wilson, R. J. Sewell, D. Smale, and W. A. Watters (1989). Cretaceous and Cenozoic sedimentary basins and geological evolution of the Canterbury region, South Island, New Zealand. *New Zealand Geological Survey Basin Studies 2*. Wellington, New Zealand: Department of Scientific and Industrial Research, 94 pp. + enclosures.

Forsyth, P. J. (2001). *Geology of the Waitaki Area*. Institute of Geological and Nuclear Sciences 1:250,000 geological map 19, 1 sheet and 64 pp. Lower Hutt, New Zealand: GNS Science.

Forsyth, P. J., D. J. A. Barrell, and R. Jongens (2008). *Geology of the Christchurch Area*. Institute of Geological and Nuclear Sciences 1:250,000 geological map 16, 1 sheet and 67 pp. Lower Hutt, New Zealand: GNS Science.

Fry, B., and M. C. Gerstenberger (2011). Large apparent stresses from the Canterbury earthquakes of 2010 and 2011. *Seismological Research Letters* **82**, 833–838.

Fukuyama, E., W. L. Ellsworth, F. Waldhauser, and A. Kubo (2003). Detailed fault structure of the 2000 Western Tottori, Japan, earthquake sequence. *Bulletin of the Seismological Society of America* **93**, 1,468–1,478.

Gledhill, K., J. Ristau, M. Reyners, B. Fry, and C. Holden (2011). The Darfield (Canterbury, New Zealand) M_w 7.1 earthquake of 4 September 2010: A preliminary seismological report. *Seismological Research Letters* **82**, 378–386.

Hicks, S. R. (1989). *Structure of the Canterbury Plains, New Zealand, from gravity modelling*. Research Report 222, Geophysics Division, Department of Scientific and Industrial Research, Wellington, New Zealand.

Keiding, M., B. Lund, and T. Árnadóttir (2009). Earthquakes, stress, and strain along an obliquely divergent plate boundary: Reykjanes Peninsula, southwest Iceland. *Journal of Geophysical Research* **114**, B09306; doi:10.1029/2008JB006253.

Laird, M. G., and J. D. Bradshaw (2004). The break-up of a long-term relationship: The Cretaceous separation of New Zealand from Gondwana. *Gondwana Research* **7**, 273–286.

Leitner, B., D. Eberhart-Phillips, H. Anderson, and J. Nabelek (2001). A focused look at the Alpine fault, New Zealand: Seismicity, focal mechanisms and stress observations. *Journal of Geophysical Research* **106**, 2,193–2,220.

Mogg, W. G., K. Aurisch, R. O'Leary, and G. P. Pass (2008). The Carrack-Caravel prospect complex: A possible sleeping giant in the deep Canterbury Basin, New Zealand. *Proceedings of the Petroleum Exploration Society of Australia Eastern Australasian Basins Symposium III*, Sydney, Australia, 14–17 September 2008, 369–378.

Mount, V. S., and J. Suppe (1987). State of stress near the San Andreas fault. *Geology* **15**, 1,143–1,146.

Pearson, C. (1994). Geodetic strain determinations from the Okarito and Godley-Tekapo regions, central South Island, New Zealand. *New Zealand Journal of Geology and Geophysics* **37**, 309–318.

Pearson, C., J. Beavan, D. Darby, G. H. Blick, and R. I. Walcott (1995). Strain distribution across the Australian-Pacific plate boundary in the central South Island, New Zealand, from 1992 GPS and earlier terrestrial observations. *Journal of Geophysical Research* **100**, 22,071–22,081.

Quigley, M., P. Villamor, K. Furlong, J. Beavan, R. Van Dissen, N. Litchfield, T. Stahl, B. Duffy, E. Bilderback, D. Noble, D. Barrell, R. Jongens, and S. Cox (2010). Previously unknown fault shakes New Zealand's South Island. *Eos, Transactions, American Geophysical Union* **91**, 469–472.

Rattenbury, M. S., D. B. Townsend, and M. R. Johnston (2006). *Geology of the Kaikoura Area*. Institute of Geological and Nuclear Sciences 1:250,000 geological map 13, 1 sheet and 70 pp. Lower Hutt, New Zealand: GNS Science.

Robinson, R., and P. J. McGinty (2000). The enigma of the Arthur's Pass, New Zealand, earthquake. 2. The aftershock distribution and its relation to regional and induced stress fields. *Journal of Geophysical Research* **105**, 16,139–16,150.

Sibson, R. H. (1985). A note on fault reactivation. *Journal of Structural Geology* **7**, 751–754.

Sibson, R. H. (1986). Rupture interaction with fault jogs. In *Earthquake Source Mechanics*, ed. S. Das, J. Boatwright, and C. H. Scholz, 157–167. American Geophysical Union Monograph 37 (Maurice Ewing Series 6). Washington, DC: American Geophysical Union.

Sibson, R. H., F. C. Ghisetti, and R. A. Crookbain (forthcoming). "Andersonian" wrench faulting in a regional stress field during the 2010–2011 Canterbury, New Zealand, earthquake sequence. In *Stress Controls on Faulting, Fracturing and Igneous Intrusion in the Earth's Crust—Commemorating the Work of Ernest Masson Anderson*, ed. D. Healy *et al.* Geological Society of London special publication.

Thatcher, W., and D. P. Hill (1991). Fault orientations in extensional and conjugate strike-slip environments and their implications. *Geology* **19**, 1,116–1,120.

Wallace, L. M., J. Beavan, R. McCaffrey, K. Berryman, and P. Denys (2007). Balancing the plate motion budget in the South Island, New Zealand, using GPS, geological and seismological data. *Geophysical Journal International* **168**, 332–352.

Wesnousky, S. G. (1988). Seismological and structural evolution of strike-slip faults. *Nature* **335**, 340–343.

Department of Geology
University of Otago
P.O. Box 56
Dunedin 9054, New Zealand
rick.sibson@otago.ac.nz
(R. S.)